PHYSICAL REVIEW B VOLUME 12, NUMBER 8 15 OCTOBER 1975

Acoustic modes of the phonon dispersion relation of NbD_x alloys*

J. M. Rowe, N. Vagelatos, and J. J. Rush
Institute for Materials Research, National Bureau of Standards, Washington, D.C. 20234

H. E. Flotow
Chemistry Division, Argonne National Laboratory, Argonne, Illinois 60439
(Received 5 May 1975)

The acoustic modes of the phonon dispersion relation in Nb, $NbD_{0.15}$, and $NbD_{0.45}$ have been measured at 473 K for phonons with wave vectors along the [100], [110], and [111] axes by coherent neutron scattering. The observed neutron groups for both alloys were well defined, with little or no apparent broadening. The results are compared to similar data for Nb-Mo alloys and with previous lattice-dynamics results for $PdD_{0.63}$. This comparison shows that despite differences in detail, the general features of the dispersion relations of NbD_x and Nb-Mo are similar after allowing for the differences in lattice parameters for the two alloys. The measured dispersion curves and derived phonon frequency distributions for the Nb-D alloys are quite different from the analogous results for $PdD_{0.63}$ in that the average acoustic phonon frequencies *increase* with increasing deuterium concentration and lattice parameter.

I. INTRODUCTION

Niobium is one of a series of metals which will absorb large quantities of hydrogen or deuterium to form nonstoichiometric interstitial alloys at elevated temperatures.[1] In this interstitial-solid-solution phase, generally called the α phase, the symmetry of the host-metal atoms remains bcc as hydrogen is added, while the lattice parameter increases with hydrogen content. At lower temperatures, the phase diagram is more complicated and the α phase coexists with a noncubic β or "hydride" phase. However, for temperatures greater than about 450 K, the Nb-H system remains in the α phase for H/Nb ratios as large as 0.8–0.9. In this phase, the hydrogen diffuses rapidly through the available interstitial sites (at a rate equivalent to a macroscopic diffusion constant $\sim 10^{-5}$ cm^2/sec at 473 K) leading to an effective random partial occupation of each site. The best present evidence[2] indicates that the hydrogen occupies the "tetrahedral" sites in the bcc lattice located at $(0, \frac{1}{2}, \frac{1}{4})a$ where a is the cubic-lattice parameter. There are six inequivalent sites of this type per primitive unit cell, so that the stoichiometric form of this alloy would be NbH_6. However, such concentrations are never reached in the α phase, presumably because of the effects discussed by Switendick[3] who has calculated band structures for these systems.

Recently there has been a renewed interest in the physical properties of metal-hydrogen systems[4] with particular emphasis on the behavior of the hydrogen. There has been much less effort expended on the changes in the properties of the metal lattice, with the exception of studies of hydrogen embrittlement.[5] The only available data on the lattice dynamics of metallic metal-hydrogen alloys have come from recent coherent neutron-scattering studies of $PdH_{0.03}$,[6] and $PdD_{0.63}$.[7] The Pd lattice is fcc and the hydrogen (deuterium) is known to occupy the octahedral sites in this system. Thus the stoichiometric form of this alloy is PdH (PdD) which has the sodium-chloride structure and is a superconductor with high T_c (~9 K for PdH and 11 K for PdD). The band structure of this alloy has been calculated by Switendick,[8] and the neutron-scattering results for the optic modes of $PdD_{0.63}$ confirmed the existence of a large second-like-neighbor D-D interaction predicted from the band-structure results. The shape of the acoustic-mode dispersion curves of $PdD_{0.63}$ were shown to be largely unaffected by the addition of D, except for a general softening which is entirely consistent with the observed lattice expansion and the fact that the lattice dynamics of Pd are dominated by near-neighbor overlap forces.

The gross features of the phonon dispersion relation in Nb are also known[9–11] to be dominated by near-neighbor forces (the first- and second-neighbor interactions are nearly an order of magnitude larger than most other forces in a Born–Von Kármán analysis). However, the Nb dispersion curves also show evidence of a strong electron-phonon interaction leading to several "kinks" or anomalies in various branches of the dispersion relation. Further, neutron-scattering measurements of Nb-Mo alloys[12] have shown that the addition of Mo to Nb changes the anomalies in a way consistent with a rigid-band model for the band structure of these substitutional alloys. The present experiment was undertaken to study the behavior of the acoustic modes in NbD_x (which are dominated by metal-atom motions) as a function of deuterium concentration. The optic modes, which should have energies above 70 meV,[13,14] were not measured in the present experiments. Since the highest acoustic modes have energies of approximately 27 meV, the optic modes are not expected to interact strongly with the acoustic modes.

It is obvious that it is inherently difficult to compare lattice dynamics results for interstitial (NbD_x) and substitutional (Nb_xMo_{1-x}) alloys directly. In spite of this difficulty, it is hoped that such a comparison and a further comparison and contrast with the $PdD_{0.63}$ results will lead to an increased understanding of the bcc metal-hydrogen systems.

II. EXPERIMENTAL DETAILS

In the absence of detailed information on the phase diagram of NbD_x, we have assumed that it is similar to that for NbH_x.[2] This phase diagram shows that for temperatures greater than 445 K, the α phase is stable for H/Nb ratios as great as 0.8, but that for lower temperatures, a two-phase region exists. Thus we have maintained the samples at temperatures greater than 473 K throughout both the sample preparation and measurements.

The $NbD_{0.15}$ and $NbD_{0.45}$ samples were prepared by allowing pure deuterium gas ($H/D < 0.005$) to react with a single crystal of niobium at 723 K. The original niobium crystal was in the form of a cylinder 1.2 cm in diameter by 5.0-cm long oriented with a [100] crystal axis along the cylinder axis. The deuterium gas was obtained by the decomposition of a known amount of UD_3, and the amount of deuterium which reacted was determined volumetrically. The nominal compositions prepared were $NbD_{0.15\pm0.01}$ and $NbD_{0.50\pm0.05}$. This latter concentration was checked by extracting the deuterium after the completion of the experiment and the D/Nb ratio was found to be 0.448 ± 0.001. After both loadings, the sample was cooled to 473 K for the measurements.

The samples were mounted with the cylinder axis 45° from vertical to put a [110] crystal axis vertical. The lattice parameters and mosaic spreads of the sample were determined by the measurement of Bragg-peak rocking curves on the neutron spectrometer. For both samples, the mosaic spread was determined to be less than 0.4° full width at half-maximum (FWHM), and no evidence of crystal damage other than the increase of the mosaic spread from 0.2° FWHM was noted upon deuteration. The lattice parameters of the two alloys at 475 K were determined to be 3.326 ± 0.015 and 3.384 ± 0.004 Å for $NbD_{0.15}$ and $NbD_{0.45}$, respectively, in fair agreement with the results of Albrecht *et al.*[15] for NbH_x at 200 °C.

The data were taken on the BT-9 triple-axis spectrometer at the NBS reactor using a fixed incident energy of 55.0 meV. The (002) planes of a pyrolitic graphite crystal with a mosaic spread of 0.4° were used to select the incident energy, and the (004) planes of a pyrolitic graphite crystal with a mosaic spread of 0.6° were used to select the scattered energy. The angular collimations used were $\frac{2}{3}$° between the reactor and monochromator, $\frac{1}{3}$° between the monochromator and sample, $\frac{2}{3}$° between the sample and analyzer, and 1° between the analyzer and detector. The "constant-Q" technique[16] was used for the measurements, mostly with neutron energy loss, although some groups were remeasured with neutron energy gain as a check on the spectrometer calibration.

In addition, a single crystal of Nb in the form of a cylinder 0.8 cm in diameter by 5.0-cm long with a [110] crystal axis parallel to the cylinder axis was used to measure the dispersion relation for Nb at 473 K for comparison with the alloy data.

Data were taken for phonons propagating along the [100], [111], and [110] axes of all three samples. For the [110] branch, only one transverse mode (with polarization vector in a [001] direction) was measured since the other branch is polarized perpendicular to the scattering plane used.

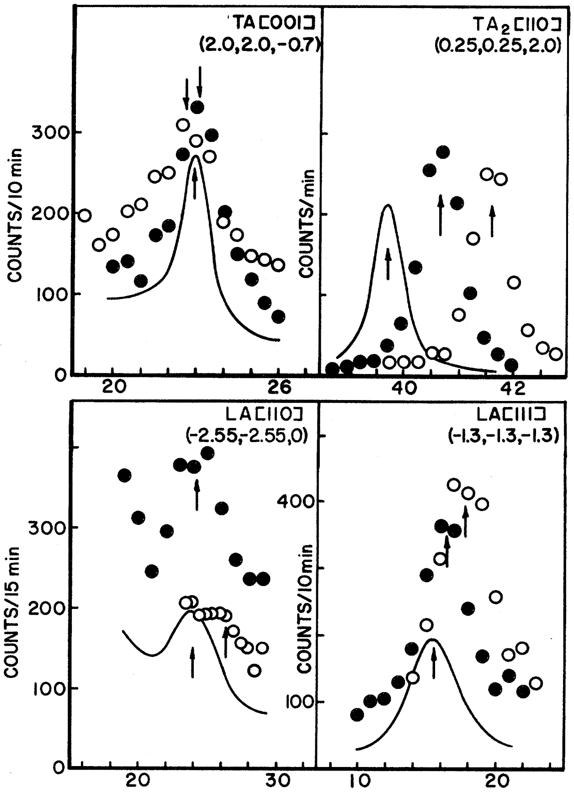

FIG. 1. Typical acoustic neutron groups observed in Nb (solid line), $NbD_{0.15}$ (full circles), and $NbD_{0.45}$ (open circles. The corresponding phonon polarization and wave vector, as well as the neutron wave-vector transfer $\vec{Q}$ are given.

TABLE I. Experimental normal-mode energies of Nb, $NbD_{0.15}$, and $NbD_{0.448}$ at 200 °C (in meV).

q/q_{max}	[001]T Nb	[001]T $NbD_{0.15}$	[001]T $NbD_{0.45}$	[001]L Nb	[001]L $NbD_{0.15}$	[001]L $NbD_{0.45}$
0.1				7.45 ± 0.44	7.15 ± 0.44	6.75 ± 0.15
0.2	4.20 ± 0.26	4.75 ± 0.26	5.55 ± 0.08	13.00 ± 0.34	13.10 ± 0.34	13.00 ± 0.15
0.3	6.70 ± 0.26	7.50 ± 0.26	8.65 ± 0.10	18.20 ± 0.35	18.45 ± 0.40	18.50 ± 0.50
0.4	10.50 ± 0.30	11.20 ± 0.20	12.50 ± 0.20	23.0 ± 0.30	22.70 ± 0.30	22.70 ± 0.35
0.5	14.50 ± 0.25	15.30 ± 0.25	15.90 ± 0.20	23.80 ± 0.30	23.70 ± 0.50	25.80 ± 0.40
0.6	19.05 ± 0.20	19.60 ± 0.20	19.60 ± 0.25	23.40 ± 0.35	23.40 ± 0.40	25.00 ± 0.60
0.7	22.95 ± 0.25	23.10 ± 0.25	22.65 ± 0.25	23.40 ± 0.35	23.00 ± 0.40	23.90 ± 0.70
0.8	25.30 ± 0.30	25.50 ± 0.30	25.00 ± 0.30	24.10 ± 0.35	23.30 ± 0.40	24.50 ± 0.30
0.9	26.85 ± 0.30	26.50 ± 0.30	26.20 ± 0.30	26.15 ± 0.30	26.00 ± 0.40	26.00 ± 0.30
1.0	27.15 ± 0.30	27.00 ± 0.50	27.10 ± 0.50	27.15 ± 0.30	26,80 ± 0.50	27.10 ± 0.50
		[111]T			[111]L	
0.1	4.85 ± 0.26	5.15 ± 0.23	5.30 ± 0.10	10.05 ± 0.32	10.55 ± 0.35	10.75 ± 0.20
0.15	6.98 ± 0.26	7.63 ± 0.26	8.55 ± 0.15			
0.2	9.40 ± 0.30	10.35 ± 0.30	11.35 ± 0.15	18.50 ± 0.30	19.15 ± 0.30	19.30 ± 0.50
0.3	13.75 ± 0.25	15.25 ± 0.25	16.85 ± 0.20	23.95 ± 0.20	23.90 ± 0.30	26.10 ± 0.40
0.4	18.55 ± 0.25	19.30 ± 0.25	20.15 ± 0.50	22.75 ± 0.30	23.00 ± 0.40	25.40 ± 0.40
0.45				21.60 ± 0.30	22.30 ± 0.40	
0.5	20.50 ± 0.30	21.35 ± 0.30	22.00 ± 0.50	20.80 ± 0.30	21.70 ± 0.40	22.00 ± 0.50
0.55				19.85 ± 0.20	20.30 ± 0.30	
0.6	21.40 ± 0.50	22.50 ± 0.50	23.00 ± 0.50	18.00 ± 0.50	19.00 ± 0.35	19.75 ± 0.40
0.7	21.50 ± 0.40	23.00 ± 0.30	23.65 ± 0.30	15.50 ± 0.40	16.40 ± 0.30	17.80 ± 0.40
0.8	23.80 ± 0.40	24.00 ± 0.30	25.00 ± 0.30	18.10 ± 0.40	18.20 ± 0.40	19.15 ± 0.40
0.9	26.40 ± 0.30	26.10 ± 0.30	26.80 ± 0.50	24.40 ± 0.60	24.50 ± 0.50	23.90 ± 0.30
1.0	27.15 ± 0.30	27.00 ± 0.50	27.10 ± 0.50	27.15 ± 0.30	27.00 ± 0.50	27.10 ± 0.50
		$[110]T_2$			[110]L	
0.1	3.25 ± 0.24	3.80 ± 0.42		8.85 ± 0.45	8.90 ± 0.35	9.00 ± 0.10
0.15	5.00 ± 0.21	5.75 ± 0.21	6.65 ± 0.10			
0.2	7.10 ± 0.16	8.00 ± 0.15	8.60 ± 0.10	16.05 ± 0.30	16.20 ± 0.30	16.90 ± 0.30
0.25	9.70 ± 0.16	10.65 ± 0.21	11.60 ± 0.10	18.90 ± 0.25	19.75 ± 0.40	20.15 ± 0.60
0.3	12.55 ± 0.16	13.55 ± 0.21	14.40 ± 0.10	20.80 ± 0.40	21.70 ± 0.40	22.30 ± 0.25
0.35	15.80 ± 0.10	16.65 ± 0.15	17.00 ± 0.10	21.70 ± 0.40	22.40 ± 0.40	24.20 ± 0.50
0.4	18.50 ± 0.10	19.25 ± 0.20	19.50 ± 0.10	22.40 ± 0.30	23.40 ± 0.50	25.45 ± 0.50
0.45	20.45 ± 0.20	20.80 ± 0.30	21.40 ± 0.40	23.90 ± 0.40	24.20 ± 0.40	26.25 ± 0.50
0.5	21.05 ± 0.30	21.80 ± 0.50	22.10 ± 0.50	24.00 ± 0.35	24.60 ± 0.50	26.20 ± 0.50

III. RESULTS

Several typical neutron groups are shown in Fig. 1 for Nb, $NbD_{0.15}$, and $NbD_{0.45}$ at 473 K. The shifts in phonon energies are clearly visible in this figure, and the increasing "background" in the series Nb, $NbD_{0.15}$, $NbD_{0.45}$ is also obvious. This background represents incoherent scattering from D (the ratio of incoherent/coherent scattering cross sections for deuterium is 2.0/5.4) and disorder scattering arising from the nonstoichiometry of the alloys. As can be seen from the figure, there is no observable broadening of the neutron-scattering peaks in the $NbD_{0.15}$ alloy, although there may be some increased width for the higher-concentration alloy. However, the resolution used in the present experiment was not adequate to obtain quantitative measurements of this effect. Well-defined neutron groups were observed for all wave vectors for both alloys.

The phonon energies measured are listed in Table I, where the assigned errors represent estimates of 95% confidence limits rather than standard deviations. The data for low-energy phonons near the zone center have been corrected for energy shifts due to resolution effects (primarily vertical resolution). These corrections were determined empirically by remeasuring the Nb phonons at much better resolution and using the results to correct the alloy data.

The final results are also presented graphically in Fig. 2, where the results for pure Nb at 473 K are represented by solid lines in order to make the figure easier to follow. These solid lines are the result of hand-drawn curves rather than the fit to the data described in a later section. Several interesting features of the present results are apparent from this figure.

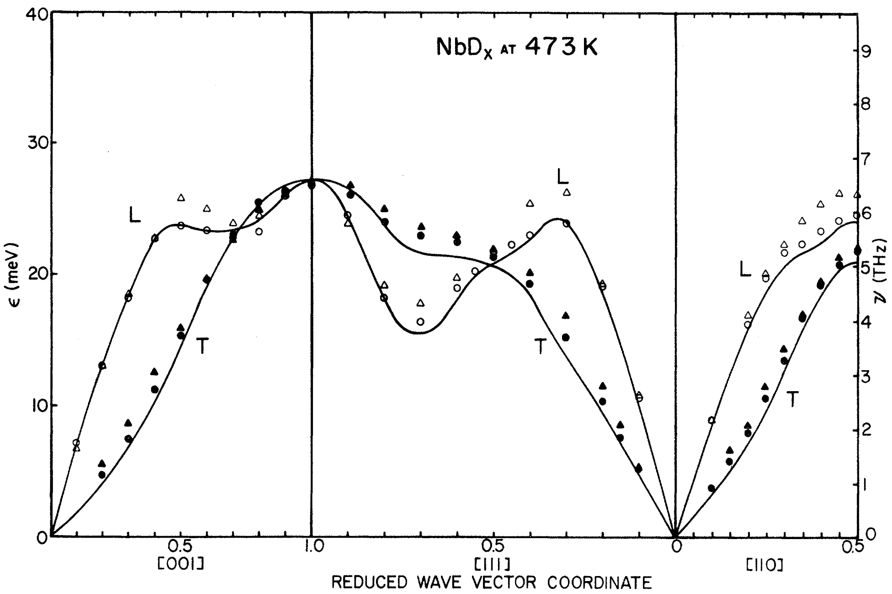

FIG. 2. Phonon-dispersion data for Nb (solid line), $NbD_{0.15}$ (full and open circles), and $NbD_{0.45}$ (full and open triangles). Error bars are omitted for clarity.

(i) The marked positive dispersion in the [100]T and [110]T branches of pure Nb at room temperature and at 473 K is progressively reduced as deuterium is added to the metal. It should also be noted that the present results for pure Nb are in good agreement with an intepolation of the temperature dependence of pure Nb measured by Powell *et al.*,[17] which showed that increasing temperature also reduced the positive dispersion in pure Nb. (ii) The dip in the [100]L branch near $\zeta(aq_x/2\pi)=0.7$ persists even in the $NbD_{0.45}$ results. (iii) The "kink" in the [110]L branch near $\zeta=0.35$ is present in the $NbD_{0.15}$ results but has disappeared for $NbD_{0.45}$. (iv) The shape of the [111] branches of $NbD_{0.45}$ are changed considerably from those of $NbD_{0.15}$ and Nb. In particular, the "kink" near $\zeta=0.5$–0.6 has essentially disappeared in the high-concentration alloy, while the height of the minimum near $\zeta=0.7$ increases with D content. (v) Finally, and perhaps most striking of all, the overall frequencies tend to *increase* as deuterium is added, even though the lattice parameter increases by more than 2% in going from Nb to $NbD_{0.45}$. Since the overall scale of the phonon energies in Nb is dominated by short-range repulsive interactions, this result is not expected. Note that if an interaction with the optic modes (Nb-D coupling) were important, it would tend to lower the highest acoustic-mode energies.

The present results have been fitted to a general sixth-nearest-neighbor tensor force Born–Von Kármán model of the type used by Nakagawa and Woods[9] for pure Nb. The resultant parameters are given in Table II. We believe that these parameters give a reasonable representation of the phonon energies in unmeasured areas of reciprocal space (although, of course, the models do *not* reproduce exactly the kinks in the dispersion curves). We have used these models to derive phonon frequency distributions using the technique of Gilat and Raubenheimer[18] with the result shown in Fig. 3. It has previously been demonstrated[19] that the multiparameter Born–Von Kármán model does not necessarily predict with high accuracy the phonon dispersion relations in off-symmetry directions. Therefore, the fine structure of the density of states in Fig. 3 (e.g., the sharpness of the maxima and the splitting of the high-energy peaks) may not be significant. However, the general features of the derived frequency distributions, including the regions of maximum phonon density, are in good agreement with the experimentally determined phonon dispersion curves in Fig. 2 and are certainly meaningful. In fact, a comparison of the $g(\nu)$'s

TABLE II. Sixth-neighbor Born–Von Kármán force constants.

Position of neighbor	$(a/2)(1,1,1)$		$(a/2)(2,0,0)$		$(a/2)(2,2,0)$			$(a/2)(3,1,1)$				$(a/2)(2,2,2)$		$(a/2)(4,0,0)$	
Force constant	1*XX*	1*XY*	2*XX*	2*YY*	3*XX*	3*ZZ*	3*XY*	4*XX*	4*YY*	4*YZ*	4*XY*	5*XX*	5*XY*	6*XX*	6*YY*
Nb	13734	9446	13440	−2242	1884	−5453	1366	3711	−465	−237[a]	1383	−944	−1753	−4548	245[a]
$NbD_{0.15}$	13725	9166	14881	−834	1880	−4505	684	3840	−700	−396[a]	1357	−1191	−923	−5072	802
$NbD_{0.45}$	13501	7213	24906	−1016	2146	−121[a]	1216	2845	−109[a]	−2036	1900	−3055	−1176	−4778	−171[a]

[a] For these parameters, the estimated uncertainty is as large as or larger than the value of the parameter.

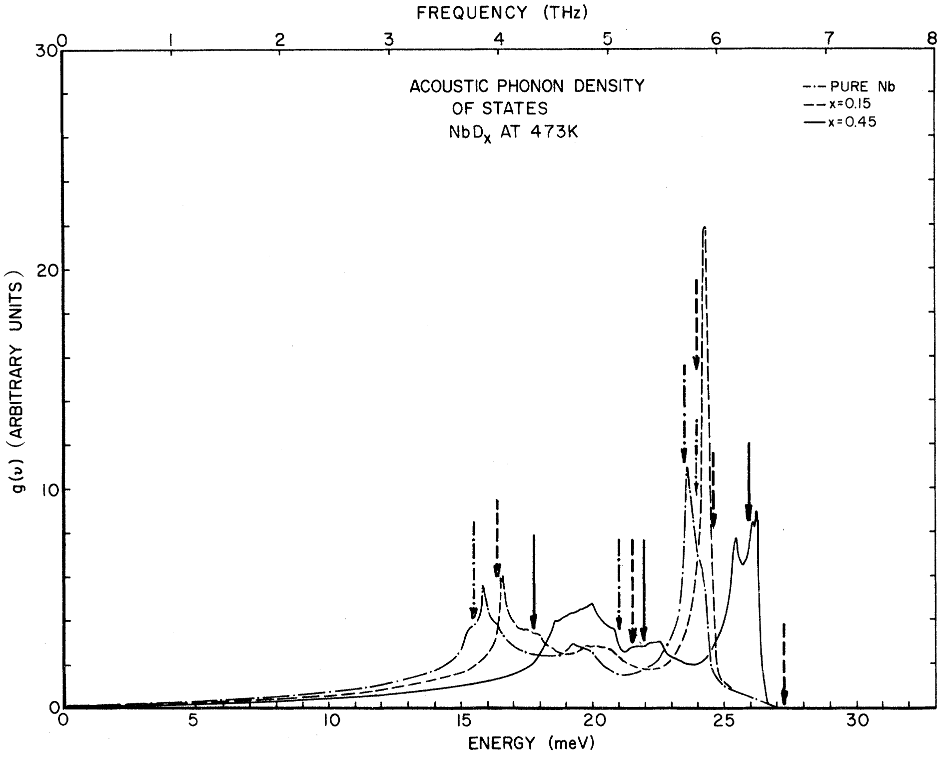

FIG. 3. Phonon density of states for Nb (dash dot dash), $NbD_{0.15}$ (dash dash dash), and $NbD_{0.45}$ (solid line). The arrows denote critical points or other points of high-phonon density suggested from the dispersion curves in Fig. 2.

obtained for niobium and the Nb-D alloys leads to several interesting observations. (i) At low energies (< 15 meV), $g(\nu)$ is lowered as the deuterium concentration is increased. (ii) As noted above, the average phonon energy (in fact, the energy of all the density-of-states maxima) increases with increasing deuterium content. (iii) The *maximum* phonon energy is independent of the deuterium content.

IV. DISCUSSION

Unfortunately, there is no useful general model upon which to base the discussion of the present results. Various authors[20–23] have addressed different aspects of the lattice dynamics of pure Nb from quite different points of view, but none of these treatments has yielded quantitative agreement with the measured dispersion relations. In the absence of reliable models, we shall proceed by comparing the present results to the results for Nb-Mo alloys[12] and for $PdD_{0.63}$.[7]

The Nb-rich alloys of Nb-Mo were shown to have phonon dispersion relations remarkably similar in shape to those for pure Nb, while the average energy of the phonons increased. Although this result was attributed to the details of the Fermi-surface shape and to the change in the density of states at the Fermi surface, there is little doubt that the general increase in frequencies was at least partly attributable to the continuously decreasing lattice parameters of these alloys as Mo is added. For NbD_x alloys, the average frequency shift is also positive, in spite of the *increased* lattice parameter. However, the effect is much less pronounced than for the Nb-Mo alloys, suggesting that two effects—the lattice expansion and the increasing density of states at the Fermi level—are tending to cancel each other. Thus, it appears that the rigid-band model, which explains the Nb-Mo results well, can also provide a reasonable explanation of the behavior of an NbD_x-alloy system when allowance is made for the variation of the direct interactions with lattice parameters. However, there are distinct changes in the shape of the dispersion curves of the $NbD_{0.45}$ alloy (such as the disappearance of the apparent anomaly in the [111]L branch) which are not seen in the Nb-Mo alloys of similar concentration. This implies that, as expected, the rigid-band model breaks down at high-deuterium concentrations in the Nb-D interstitial alloy.

Further, the present results for $NbD_{0.45}$ (Figs. 2 and 3) also show a much different dependence of the acoustic modes on deuterium content (and/or lattice parameter) than those for $PdD_{0.63}$,[7] in which the expansion of the metal lattice (by ~5%) lead to a (15–20)% *decrease* in the acoustic phonon energies. This is undoubtedly a reflection of the quite different nature of the forces in pure Pd and pure Nb—in particular, of the extent to which the phonon dispersion relation in Nb is related to the details of the electronic band structure rather than to the repulsive Born-Mayer forces which are dominant in Pd.

Finally, the existence of well-defined acoustic modes in $NbD_{0.45}$ which is a highly disordered system is probably a reflection of the weak coupling between the motions of the light interstitials and the heavy metal atoms.

ACKNOWLEDGMENT

We would like to thank A. Cinquepalma for his valuable technical assistance.

---

[*] Work supported in part by the U. S. Energy Research and Development Agency.

[1] R. J. Walter and W. T. Chandler, Trans. AIME 233, 762 (1965); see also C. Wert, D. O. Thompson, and O. Buck, J. Phys. Chem. Solids 31, 1973 (1970).

[2] H. D. Carstenjen and R. Sizmann, Ber. Bunsenges. Phys. Chem. 76, 1223 (1972).

[3] A. C. Switendick in *Hydrogen Energy*, *Part B*, edited by T. N. Vezeroglu (Plenum, New York, 1975), p. 201.

[4] For a reasonably complete review of recent work on metal hydrides, see the Proceedings of the International Meeting on Hydrogen in Metals, Julich, Germany (1972), published in Ber. Bunsenges. Phys. Chem. 76, 705 (1972).

[5] See, e.g., C. V. Owens and T. E. Scott, Met. Trans. 3, 1715 (1972).

[6] J. M. Rowe, J. J. Rush, and H. G. Smith, Phys. Rev. B 8, 6013 (1973).

[7] J. M. Rowe, J. J. Rush, Mark Mostoller, H. G. Smith, and H. E. Flotow, Phys. Rev. Lett. 33, 1297 (1974).

[8] A. C. Switendick, Ber. Bunsenges, Phys. Chem. 76, 535 (1972).

[9] Y. Nakagawa and A. D. B. Woods, Phys. Rev. Lett. 11, 271 (1963).

[10] Y. Nakagawa and A. D. B. Woods, in *Lattice Dynamics*, edited by R. F. Wallis (Pergamon, Oxford, 1965), p. 39.

[11] R. I. Sharp, J. Phys. C 2, 421 (1969); 2, 432 (1969).

[12] B. M. Powell, P. Martel, and A. D. B. Woods, Phys. Rev. 171, 727 (1968).

[13] H. Conrad, G. Bauer, G. Alefeld, T. Spunzer, and W. Schmatz, Z. Phys. 266, 239 (1974).

[14] S. S. Pan, M. L. Yeater, and W. E. Moore, in *Molecular Dynamics and Structure of Solids*, edited by R. S. Carter and J. J. Rush (U. S. National Bureau of Standards Special Publication 301, Washington, D. C., 1969), p. 315.

[15] W. M. Albrecht, W. D. Goode, and M. W. Mallett, J. Electrochem. Soc. 106, 981 (1959).

[16] B. N. Brockhouse in *Inelastic Scattering of Neutrons in Solids and Liquids* (International Atomic Energy Agency, Vienna, 1961), p. 113.

[17] B. M. Powell, A. D. B. Woods, and P. Martel, in *Neutron Inelastic Scattering* 1972, Proceedings of a Symposium, Grenoble, 1972 (International Atomic Energy Agency, Vienna, 1972), p. 43.

[18] G. Gilat and L. J. Raubenheimer, Phys. Rev. 44, 390 (1966).

[19] See, e.g., R. Stedman, L. Almqvist, and G. Nilsson, Phys. Rev. 162, 549 (1967); R. C. Dynes, J. P. Carbotte, and E. J. Woll, Jr., Solid State Commun. 6, 101 (1968).

[20] M. I. Korsunskii, Ya. E. Ginkin, V. I. Markovin, V. G. Zavodinskii, and V. V. Satsuk, Fiz. Tverd. Tela. 13, 2138 (1971) [Sov. Phys.-Solid State 13, 1793 (1972)].

[21] B. N. Ganguly and R. F. Wood, Phys. Rev. Lett. 28, 681 (1972).

[22] S. T. Chui, Phys. Rev. B 9, 3300 (1974).

[23] W. Weber, Ph.D. thesis (Techischen Universität München, 1972) (unpublished).